POLITECNICO DI TORINO
Repository ISTITUZIONALE

Lithium fluoride coloration by laser-plasma soft x-rays: A promising tool for X-ray microscopy and photonics

(Article begins on next page)

20 April 2024

Lithium fluoride coloration by laser-plasma soft X-rays: a promising tool for X-ray microscopy and photonics

Francesco Flora [*a], Giuseppe Baldacchini [a], Francesca Bonfigli [a], Antonella Lai [a], Tiziana Marolo [a], Luca Mezi [a], Rosa Maria Montereali [a], Daniele Murra [a], Nicola Lisi [b], Enrico Nichelatti [b], Anatoly Ya. Faenov [c], Tatiana A. Pikuz [c], Libero Palladino [d], Armando Reale [d], Antonio Ritucci [d], Lucia Reale [d], Giuseppe Tomassetti [d], Pasquale Fabi [e], and Tania Limongi [e].

[a]ENEA, UTS Tecn. Fis. Avanzate (FIS), C.R. Frascati, Via E. Fermi 45, 00044 Fracati, Roma, Italy;
[b]ENEA, UTS FIS, C.R. Casaccia, Via Anguillarese 301, 00060 Santa Maria di Galeria, Roma, Italy;
[c]MISDC of VNIIFTRI, Mendeleevo, Moscow Region, 141570, Russia;
[d]Università de L'Aquila e INFN, Dip. di Fisica, Coppito, L'Aquila, Italy;
[e]Università de L'Aquila e INFN, Dip. di Biologia, Coppito, L'Aquila, Italy

ABSTRACT

A new imaging detector for EUV or soft-X-ray radiation based on optically stimulated luminescence (OSL) of lithium fluoride (LiF) films or crystals is presented.
The first micro-radiography images of biological samples and of meshes obtained on LiF using a laser-plasma source or an X-ray laser are shown, and (up to now) a resolution better than one micron is demonstrated. The dependence of the coloration density vs the deposited X-ray dose is considered and the advantages of this new diagnostic technique for both coherent and non-coherent EUV sources, compared with CCDs detectors, photographic films and photoresists are discussed. This new detector is extremely suitable for laser plasmas and for X-ray lasers sources.

Keywords: EUV radiation, X-ray detectors, lithium fluoride, X-ray microscopy, imaging.

1. INTRODUCTION

Since many decades physicists discovered that ionizing radiation like UV, EUV (Extreme Ultra-Violet), X-rays, γ-rays, electron beams, etc., can generate color centers (CCs) in alkali halide crystals[1]. The physics of CCs formation is still under investigation but it is already well known that they are formed from anion vacancies occupied by electrons. CCs can absorb light in specific spectral ranges so that the crystals appear to be colored (for this reason they are called color centers). In particular, in lithium-fluoride salt (LiF) several types of CCs (like the F_2 and F_3^+ type) can re-emit visible light when excited by blue light and, after being generated, they remain stable for a very long time (centuries) even at room temperature[2]. Furthermore the excited CCs can reach the population inversion, so that the crystal can become a high gain active medium for solid state lasers.

Among the alkali halide crystals, LiF plays a unique role for different reasons: it is almost insoluble in water (just 0.13 g / 100g H_2O solubility, more than 300 times less than for NaCl), the cation-anion distance is the shortest, the Li^+ and F^- ions possess the smallest radius among the alkali and halide ions, respectively; the Knupp hardness is relatively high (99 Kg/mm^2, just two orders of magnitude less than for diamond), it can be deposited as a film by evaporation, the refraction index (n=1.3912) is one of the lowest and the band-gap (~ 14 eV) is the largest among all other alkali halides or dielectric materials in general. Furthermore, as previously mentioned, only in LiF the CCs are very stable at room temperature after being generated by any kind of ionizing radiation and several of them are luminescent in the visible spectrum.

* flora@frascati.enea.it; Phone ++39-06-94005745; fax: ++39-06-94005334;
http://www.frascati.enea.it/fis/lac/excimer/index-exc.html

For these reasons LiF, in the form of bulk or film, is interesting for many applications like optical memories[2], miniaturized optical devices as broad-band optical emitters[3] and active waveguides[4], microcavities[5] and point light sources[6,7].

The increasing demand for low-dimensionality photonic devices imposes the utilization of low penetrating radiation like low energy electron beams[2]. Recently also the use of EUV or soft X-rays has been proposed [8]. This radiation, when produced by high peak power sources like laser plasmas or discharge plasmas or X-ray lasers, can very efficiently produce the CCs as shown in the following; furthermore, being the penetration depth in the matter (in LiF for example) very short, a high spatial resolution can be achieved. On this regard, the emerging technologies presently investigated in the field of EUV lithography well combine with the research on LiF coloration by EUV irradiation with bright sources, and they potentially allow to push the spatial resolution to values below 100 nm[2,9,10]. So the old research on LiF crystals coloration by ionizing radiation is gaining more and more interest in the scientific and industrial fields[11].

In the following we show how the EUV radiation produced by a laser plasma source or by an X-ray laser can efficiently create high resolution luminescent patterns on large areas and how this combined use of laser plasma sources and LiF films as sensitive radiation detectors can improve the performances of soft X-ray microscopy and micro-radiography.

2. COLORATION OF LiF BY EUV

The photon energy of EUV radiation (20<hν<200 eV) and soft X-rays (0.2<hν<8 keV) is larger than the above mentioned LiF band-gap energy (and of any other alkali halide) and hence it is sufficient to generate CCs in LiF.

Figure 1 shows how the primary CCs (i.e. the F-type or, in other words, anion vacancies filled by one electron) can be generated by ionizing radiation; the F-centers formation process includes non-linear effects so that the centers formation efficiency is enhanced for high flux values of the ionizing radiation. This is one of the crucial points which give to bright sources (like laser plasmas) a big advantage for colorizing compared with X-ray tubes or other sources. Figure 2 shows the structure of the F-defect and of the F_2 and the F_3 ones, consisting of two and three neighboring F-centers , respectively. There exist many kinds of electronic defects, and several of them, the F_2 and F_3^+ centers, can emit in the visible range when excited in the blue region, as shown in Fig. 3, and have a quantum efficiency close to unity[11].
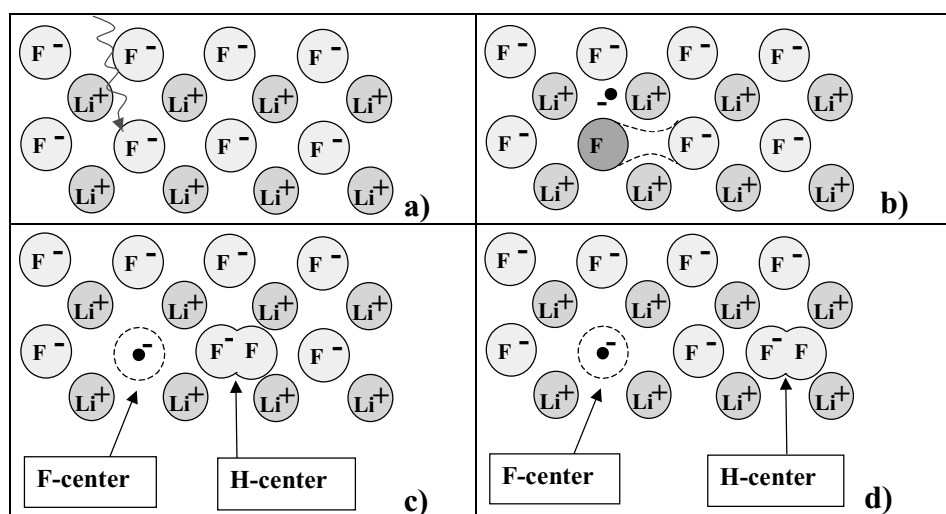

Figure 1: Formation of a Frenkel couple (centers F and H) in LiF. One or more photons ionize one fluorine atom making it neutral or positively charged (a). Then the F (or F^+) atom is rejected by the neighboring Li^+ and attracted by a neighboring F^- (b). So the F (or F^+) atom moves creating an "H-center" plus a vacancy; this vacancy immediately hosts an electron, becoming an "F-center" (c). Thermal shaking increases the gap between F and H centers (d). Neighboring F-centers can aggregate each other to form F_2 or F_3 or F_3^+ centers .

In the colored volumes of a LiF crystal even the refractive index is significantly changed [3,11]. In principle the color center density could reach values close to the atoms one in the solid, but for densities higher than 10^{17} CCs/cm^3 the quantum efficiency of F_2 and F_3^+ CCs begins to decrease[11,12,13], going down by more than one order of magnitude at

10^{20} CCs/cm^3 as shown in Fig. 4, so that the luminescence displays a concentration quenching effect. Any ionizing radiation can generate CCs when the photon energy exceeds the band gap (14 eV for LiF) of the crystal, although for very high radiation intensities (like for pulsed lasers case) multiple photon absorption processes can lead to CCs formation even in the near UV region (that is at a photon energy of few eV). But the photon energy can also influence the population ratio among the different type of CCs. In particular EUV and soft X-rays seems to generate very efficiently F_2 and F_3^+ CCs, so that by irradiating a LiF crystal or film by such radiation it becomes strongly luminescent in the green-red region when optically excited by blue light. Furthermore, as mentioned, the CCs density increases when the EUV or soft X-rays energy deposition rate is larger. For this reason laser plasma sources or discharge sources, characterized by a high peak brightness, are extremely suitable to be used for LiF coloration. Due to their high peak power and to the short penetration depth of EUV in the material, the dose deposition rate, P, can be as high as some gigawatts per cubic centimeter.
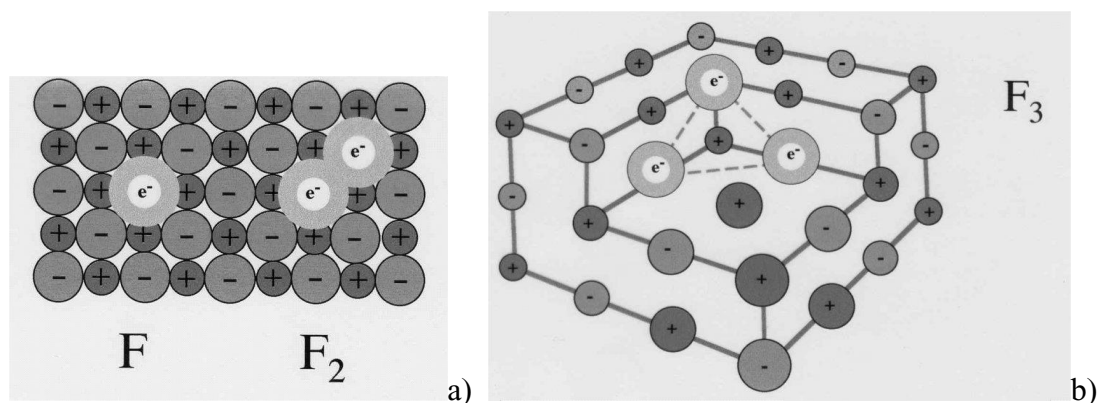

Figure 2: F-type and F_2-type color centers (a), and F_3 color centers (b)) in a alkali halide crystal. When one of the three electrons captured in the three neighboring anion vacancies (which form the F_3 center) is missing, the center is called F_3^+.
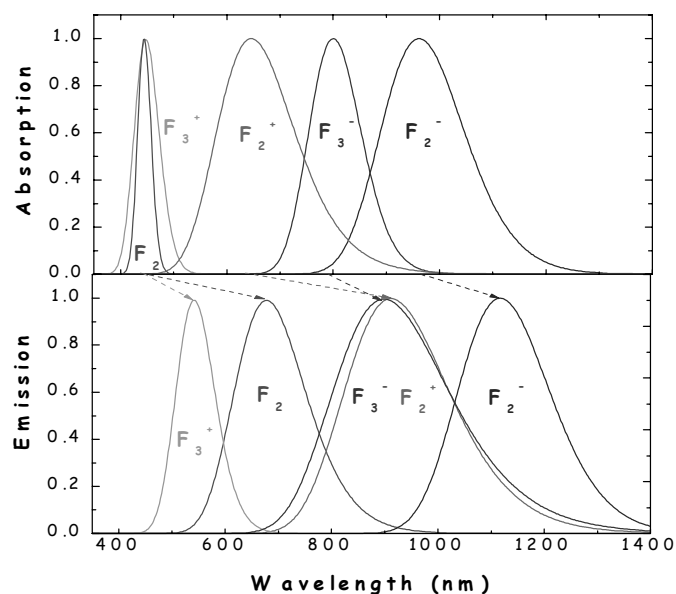

Figure 3: Absorption and emission bands of laser active aggregated color centers in LiF crystals. F_2^+ / F_3^+ centers and F_2^- / F_3^- centers are F_2 / F_3 centers having one electron missing or in excess, respectively.

The penetration depth of EUV radiation in LiF is so short that the colored layer of the material can be as thin as 20-100 nm, as shown in Fig. 5 according with Henke data[14,15].

In the present case a laser plasma source pumped by a large volume excimer laser has been used. The laser has a pulse energy ranging between 1 and 7 J and a pulse duration ranging between 10 and 120 ns[16]. The efficiency of the laser plasma is as high as 20% in the EUV, so that at 10 cm from the source the dose rate in LiF is as high as 3 GW/cm^3 and with just 1000 shots we could reach in the LiF samples a dose of some tens kJ/cm^3. After the irradiation, a CCs density in the order of 10^{19} cm^{-3} is reached in a layer of about 50 nm of the irradiated LiF samples and a strong visible photoluminescence is observed under blue light excitation.
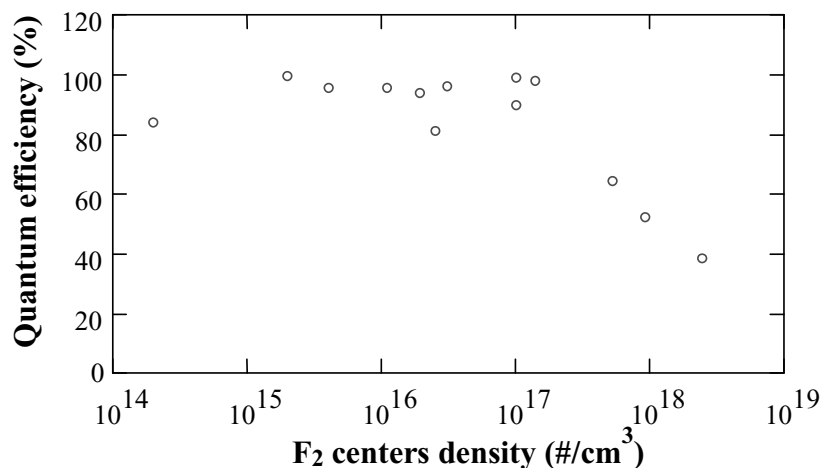

Figure 4: Quantum efficiency of F_2 centers vs their density in a LiF crystal irradiated by 3 MeV electrons. The data are from [11,12,13] and the vertical scale is normalized to the maximum value.
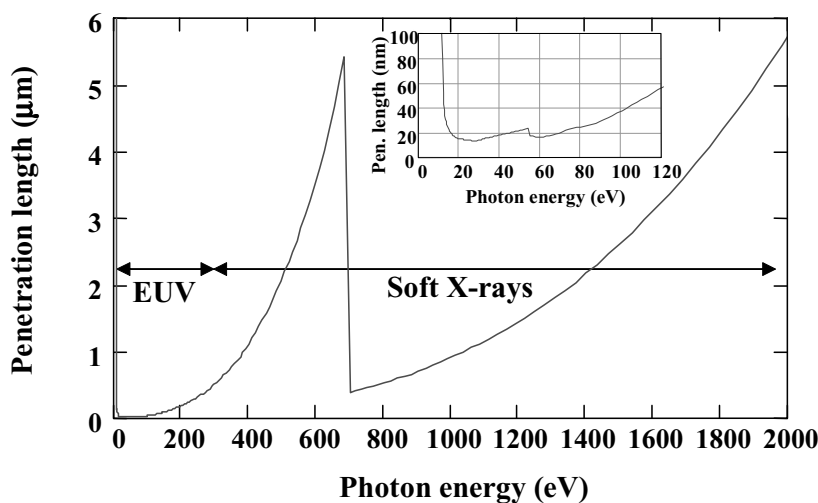

Figure 5: Penetration length of EUV and soft X-rays in LiF.

Figure 6 shows the photoluminescence image of a LiF film irradiated at different fluence values (obtained by masking the LiF surface with different polypropylene filters). Figure 7 shows the photoluminescence spectrum of the non-filtered areas of Fig.6 together with the one of a crystal exposed in the same run: the broad F_2 and F_3^+ bands can be easily recognized.

As it can be seen from Fig. 7, the formation efficiency of F_2 and F_3^+ CCs in a LiF film is one order of magnitude larger than for a LiF crystal. This effect seems to be due to the polycrystalline structure of the LiF film[17].
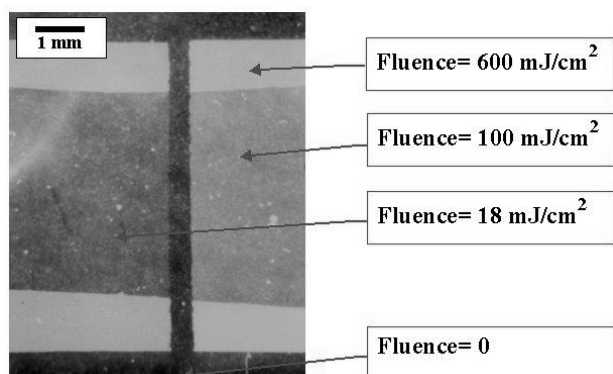

Figure 6: LiF film sample exposed to 1000 shots at 10 cm from the laser-plasma source and through a polypropylene filter step-shaped. The LiF sample is here observed in fluorescence mode, that is by exciting the sample in the blue range (at 458 nm with an Ar laser) and observing it through a yellow filter.

In LiF crystals colored by EUV the amount of F_2 and F_3^+ CCs is roughly one order of magnitude lower than that of the primary F-type centers. The dependence of the F-type CCs density in LiF from the EUV (or soft X-rays) dose and dose-rate is quadratic and logarithmic, respectively, and it is incredibly similar to that measured in other salt crystals irradiated with hard X-rays, even when the conditions change by orders of magnitude, as demonstrated in Fig. 8. In this figure the experimental values (dots) are fitted by the empirical function $F = F_0 \cdot A(P) \cdot \sqrt{\dfrac{D}{D_0}}$, where D and P are the radiation deposited dose and dose-rate, respectively, $D_0= 1$ J/cm^3 is assumed as the unity dose, $F_0 = 8 \cdot 10^{15}$ centers/cm^3 ($7.7 \cdot 10^{15}$ for NaCl) is the F-type CCs density given by a unity dose at low deposition rates ($P < P_s$), $P_s = 10$ mW/cm^3 is the threshold value of the dose rate for non-linear effects to the coloration efficiency and $A(P) = 1 + 2 \cdot \log(1 + P/P_s)$ is the efficiency enhancement function due to the non-linear effects. The experimental data for NaCl are extracted from page 221 of ref. 1.
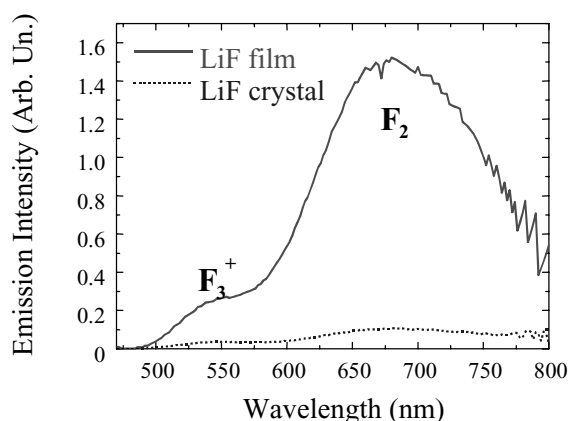

Figure 7: Photoemission spectrum of the LiF film of figure 6 (area exposed to 600 mJ/cm^2) and of a LiF crystal exposed in the same conditions, under optical pumping with the 458 nm line of an Argon laser.

As we can see, both for NaCl and for LiF the experimental values of the F-type CCs density are well fitted by the empirical parabolic function above described. This parabolic dependence of the coloration density from the X-ray dose means that the coloration efficiency (that is the CCs generated per unit dose) decreases while increasing the CCs density, as shown by the dashed line of Fig. 8b. Still our job is in progress to verify the goodness of the this empirical function for other values of dose and dose-rate. As above mentioned, it is now worthwhile to consider the big advantage of generating color centers by using laser plasmas or other bright sources: according with the first derivative of the empirical best-fit function, the coloration efficiency $\eta = \dfrac{dF}{dD} = \dfrac{F_0^2}{D_0} \cdot \dfrac{[A(P)]^2}{2 \cdot F}$ is enhanced by more than two orders of magnitude when the dose rate reaches the typical values given by laser plasmas at few centimeters from the source (roughly 10^8-10^9 W/cm^3), as illustrated in Fig. 9.
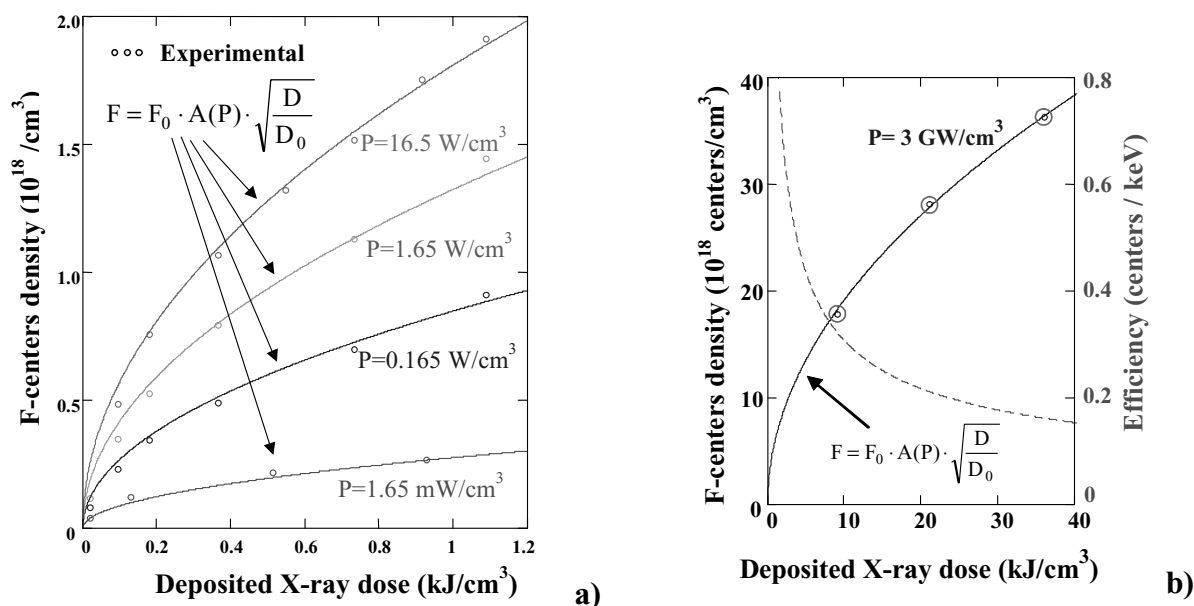

Figure 8: Experimental values (circles) and empirical best-fit function (solid lines) of the F-type CCs density vs the radiation dose deposited in a NaCl crystal with hard X-rays at different deposition rates (a) and in a LiF crystal exposed to EUV + soft-X-rays radiation at a total power deposition rate of 3 GW/cm^3 (b).
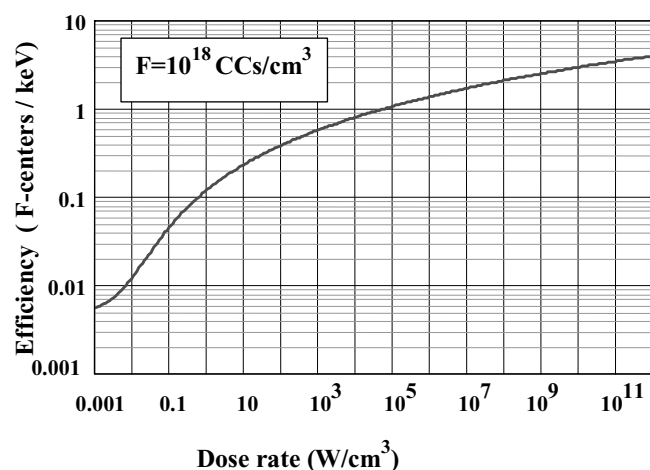

Figure 9: Coloration efficiency of soft X-rays vs deposition dose rate in LiF @ an F-type CCs density of 10^{18} CCs/cm^3. At the dose rate of laser-plasma sources (that is typically 0.1 - 1 GW/cm^3) the efficiency is more than two F-type centers per deposited keV.

3. APPLICATIONS

3.1 Application to X-ray radiography and microscopy.

It is now clear that LiF can be used as a high resolution EUV (and soft X-rays in general) detector and that its performances are unique compared with other detectors like photographic films or CCD or photoresists: the pixel size of a LiF film (that is the CCs dimension) is at atomic scale (let's say < 1nm), comparable with that of typical photoresists (i.e. < 10 nm), but at the same time the dynamic range of LiF, as deducible from Fig. 8, is orders of magnitude wider than that of photoresists. This is demonstrated in Fig. 10, where the soft X-ray radiography of a polypropylene phantom obtained on a LiF film is compared with that obtained on a Poly-Methyl-MetAchrilate (PMMA), the photoresist typically used for soft X-ray contact microscopy: on LiF the phantom fluorescence image is sharp even in zones with reduced X-ray fluence (by almost 3 orders of magnitude) while on the PMMA such zones (c and d) cannot be distinguished, nor when analyzed at visible light, neither when analyzed with an Atomic Force Microscope (AFM), which is the typical analysis for soft X-ray contact microscopy[16,18,19,20]. From this comparison it is possible also to recognize that LiF is less sensitive to dust or to the debris emitted by laser-plasmas. The PMMA has been developed for 0.5 minutes in Methyl Iso-Butyl Ketone (MIBK) developer, as usually done for X-ray microscopy[16,18,19].
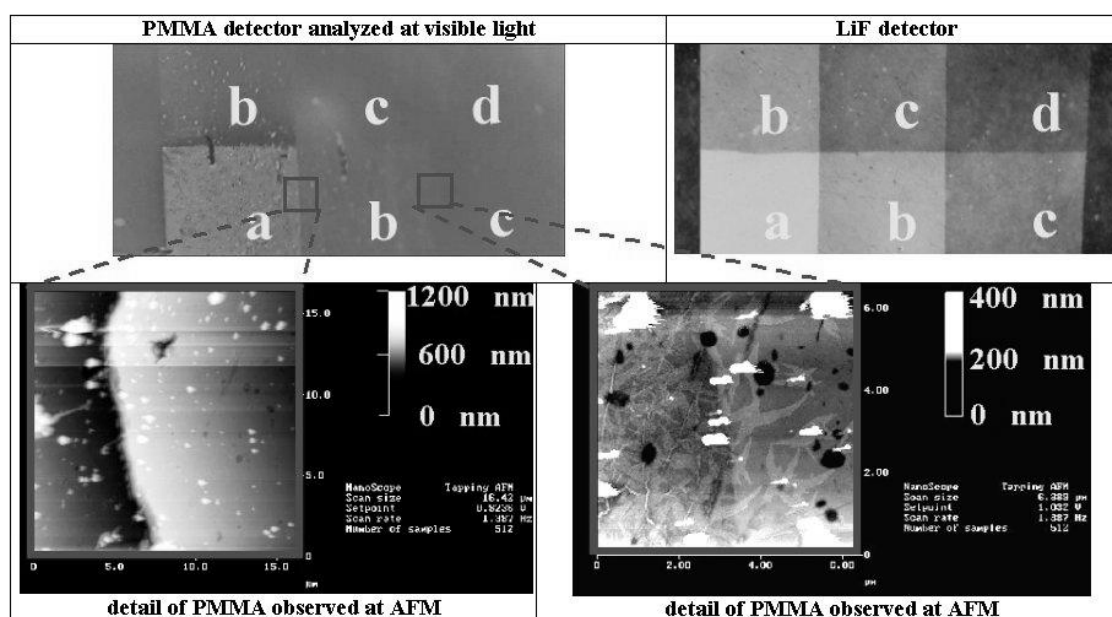

Figure 10: Radiography of a step-shaped polypropylene phantom on PMMA photoresist and on a LiF film exposed in the same conditions (600 mJ/cm^2). The phantom step-structure reduced the soft X-ray fluence by a factor 0, 150, 300 and 600 for areas a,b,c and d, respectively. The LiF sample is here analyzed in fluorescence mode (by exciting it with the 458 nm line of an Ar laser). The PMMA, after the exposure, has been developed by in MIBK. It's original thickness was 600 nm, while after development resulted (from AFM analysis as shown in the details) 200 nm for zone "a", 588 nm for zone "b" and ~600 nm for both zones "c" and "d".

The high dynamic of LiF, comparable with the photographic films one, is not the only important performance of this new detector: as for a films emulsion, even a LiF film can be deposited (by evaporation) over plastic and flexible substrates, it has no size limits, the film thickness can be varied (for example from 0.1 to few microns) to fit the penetration depth of the used radiation (see Fig. 5), it is absolutely not sensitive to visible light so that no filtering is required for radiography, and it does not need any development after the exposure; hence it can be protected (when needed) by any transparent permanent coating.

The micro-radiography on LiF of a dragonfly (*Pyrrhesoma nymphula*) wing, obtained by Optically Stimulated Luminescence (OSL) in a conventional optical microscope, is shown in Figs. 11A,B at two different magnifications. The exposure has been obtained with 1100 shots and placing the sample at 10 cm from the source. The high-contrast of the image is similar to that obtained in conventional radiographic films using the same plasma source[21], but the spatial

resolution is significantly better. For the purpose of comparison, the other wing of the same dragonfly has been exposed exactly at the same conditions onto a conventional PMMA photoresist developed, after the exposure to soft X-rays, for 30 seconds in MIBK, as usually done in X-ray microscopy[16,18,19]. After the development (i.e. after the corrosion in MIBK) a relief map of the sample is obtained on the PMMA as shown in Figs. 11c and 11d, where the PMMA is imaged with an optical microscope and an AFM, respectively. The optical image of Fig. 11C, obtained in reflection mode, is due to interference effects in the structured PMMA layer on a silicon substrate. The wing ribs (which have a diameter $\Phi \sim 20$ μm) are well visible on LiF (Fig. 11B); on the contrary, on the PMMA (Fig. 11C) the dynamic range is so poor, that it is difficult to distinguish them (the ribs are a bit whiter than the wing tissue, while the dark line at the wing border is just a diffraction effect on the highest PMMA relief step).
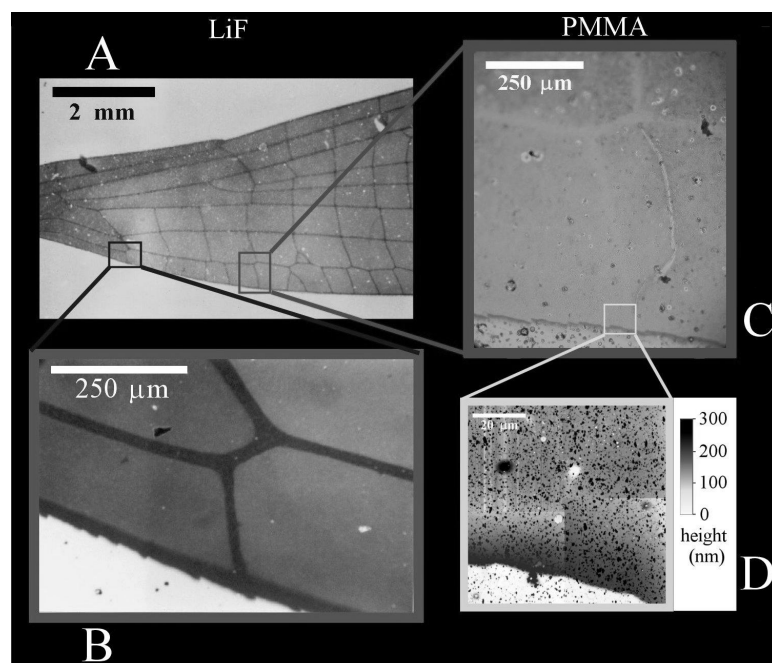

Figure 11: Micro-radiographs of a dragonfly (*Pyrrhesoma nymphula*) wing. (A) Fluorescence image of the wing obtained by exposing the sample to soft X-rays and using a LiF film as a detector. The photograph has been obtained with an optical microscope by observing the optically stimulated luminescence of the colored film. (B) An enlarged area of the same image. (C) An optical microscope photograph of the other wing, of the same dragonfly, obtained in the same experimental conditions as in Fig. 11A by using a polymeric (PMMA) photoresist film as a detector. (D) An enlarged area of the photoresist film analyzed with an atomic force microscope (a collage of four images of 40X40 μm).

Typically, the PMMA relief maps are analyzed by AFM, but in our case the spatial modulation of the PMMA surface corresponding to the ribs was so poor to be confused with the AFM noise (Fig. 11D), which is further increased by the debris (the black dots) emitted by the laser-plasma source.

These fluorescence images (as well as the following ones) are obtained by exciting the LiF sample with bue light between 400 and 490 nm and by observing it through a yellow filter transmitting between 520 and 700 nm. In this way the absorption and re-emission spectra of F_2 and F_3^+ CCs are fully matched (see Fig. 3).

In this example of X-ray micro-radiography, the sample was dry and the LiF film was uncoated. In the case of X-ray microscopy the samples are wet and alive, so they could attach rather strongly to the LiF film. In such case it might be convenient to coat the LiF with a protection layer. Figure 12 shows the first (at our knowledge) image of X-ray microscopy obtained on LiF. The biological sample is a Ciano bacteria called leptolyngbya, a green alga composed by a chain of cell having a diameter in the order of one micron. The cells are alive, in solution, and the LiF has been coated with a 50 nm layer of glass (SiO_2) which is enough transparent (T>80%) in the water-window spectral region[14,15] used for X-ray microscopy[16,18,19,20]. The resolution is significantly smaller than 1 μm but for the best performances the LiF should be analyzed by a Scanning Near-field Optical Microscope (SNOM) which was not available at the moment.
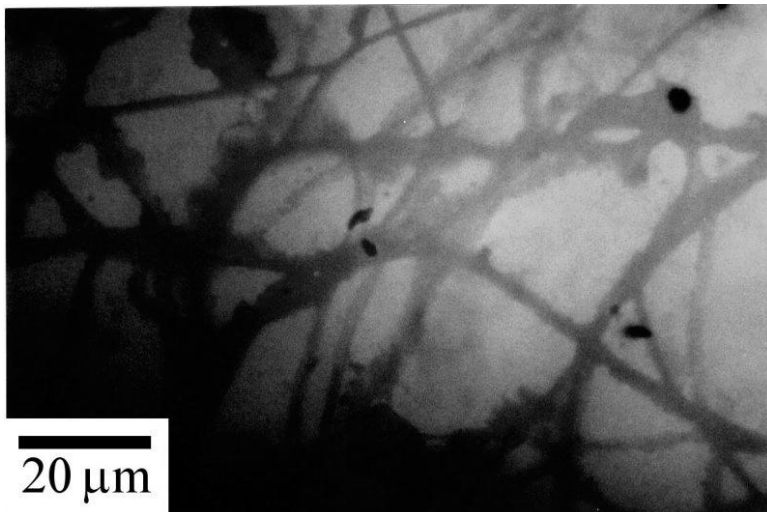
Figure 12: X-ray contact microscopy image of "leptolyngbya" cells, imaged on a 1 μm LiF film deposited (by thermal evaporation) an a Si substrate and coated (by magnetron sputtering) with a 50 nm glass layer. The image is obtained by analyzing the LiF film (after the exposure) with a fluorescence microscope having a 100X objective used in immersion (in oil) mode.

3.2 Application to X-ray laser beam detection.

The high resolution, low penetration length in the EUV and high power selectivity (see Fig. 9) makes LiF a unique and perfect detector for X-ray laser beam diagnostics. This detector can bear doses orders of magnitude larger than photographic films or CCDs, so that in some cases the laser spot can be imaged without any filtering and hence without any distortion of the intensity profile and of the phase profile.

The spot of a table top capillary discharge X-ray laser based on Ne-like Argon ions[22,23,24] has been imaged on a 1 μm LiF film both in the far-field through a 0.15 μm Al filter (Fig. 14) or directly on LiF after being brought to focus by a multilayer mirror (Fig. 15). The laser photon energy is just 26 eV but sufficient for an efficient CCs generation in LiF.
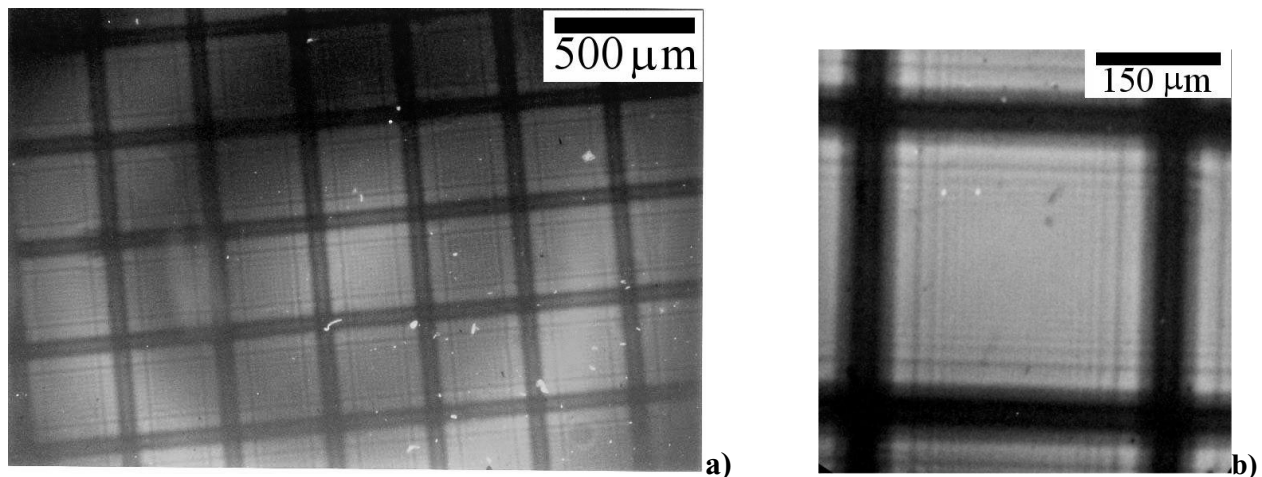

a)

b)

Figure 14: Spot of the Ar X-ray laser imaged on a LiF film through a 0.15 μm Al filter supported by a 70 lpi nickel mesh (35 laser shots). The LiF sample is at 41 cm (a) or 60 cm (b) from the capillary laser exit and the mesh is at 5 cm (a) or 3 cm (b) from the LiF film: the interference fringes of the mesh are clearly visible. The LiF samples are here observed by a fluorescence microscope with a 5X objective and a 10X objective, respectively.
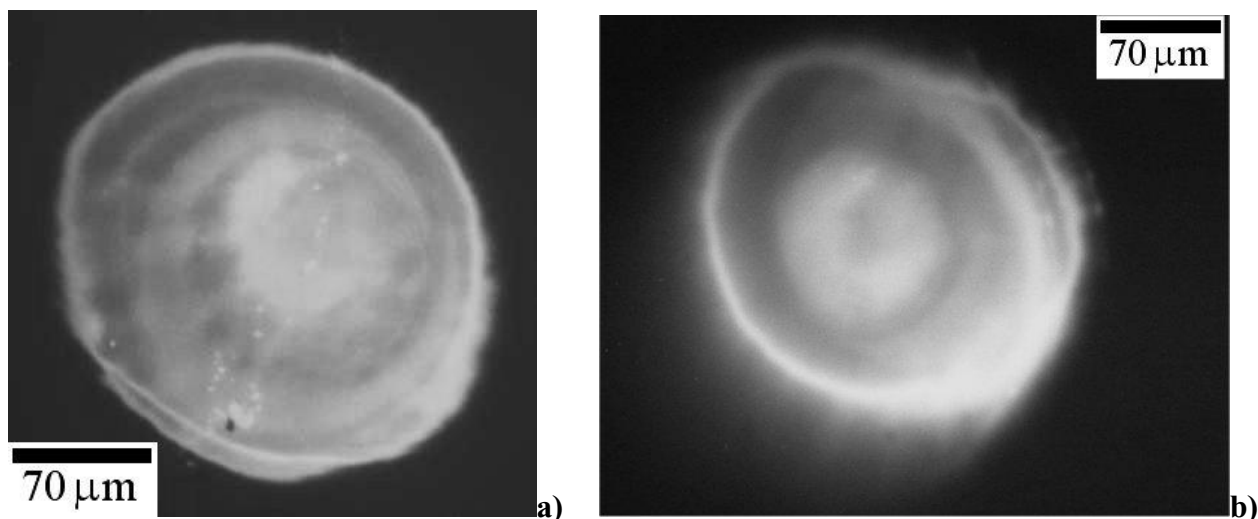
Figure 15: Spots of the Ar X-ray laser imaged on a LiF film after being focused by an f= 40 cm multilayer mirror. No filters are used. The exposure is single-shot. The LiF samples are here observed by a fluorescence microscope with a 20X objective. Small differences in the starting Ar pressure from shot-to-shot generates beam spot with different shapes (compare "a" with "b").

In the last cases the laser fluence is similar to that of Fig. 10-zone-a (i.e. around 0.5 J/cm^2) but the power density is orders of magnitude larger (almost 1 GW/cm^2) so that the LiF ablation threshold is reached and probably even the CCs luminescence quenching is reached (see Fig. 4), so that a particular care must be taken for the spot interpretation. In spite of the huge power density, still the LiF film is not destroyed. On the other hand, being the radiation penetration depth extremely short (just 15 nm according with Fig. 5) the deposition rate is as high as 10^{14} W/cm^3 and in this case the coloration efficiency is very high (Fig. 9); this improves the contrast between the laser spot with respect to the spontaneous emission background. So, in this case the non-linear effects which lead to the LiF coloration play an advantageous role for LiF compared with other detectors. The interpretation of the beam intensity distribution is still under analysis and further studies are in progress.

3.3 Generation of luminescent patterns

Most of the applications of LiF in photonics require the generation of small size (sometime sub-micrometric) colored patterns to be used as a point-like light source or as a micro-laser active medium or as a waveguide (we remind that, as above mentioned, the refraction index of the colored LiF is significantly larger than that of uncolored areas) or as optical data storage technique[2].

As a first attempt, we produced structured color patterns in LiF by placing in front of LiF films some copper meshes (in contact) and then exposing the sample to the soft X-rays and EUV radiation produced by our laser-plasma source previously described.

Figure 16 shows the radiography of a 400 lines-per-inch (lpi) copper mesh obtained on a LiF crystal. The crystal has been exposed to EUV irradiation in the same experimental conditions as in Fig. 6 (1000 shots at 10 cm from our laser plasma source above described, absorbed EUV dose ~ 30 kJ/cm^3). In this way, colored patterns are obtained on the LiF surface since the areas under the mesh structure are not colored while those which received directly the EUV radiation presents a strong luminescence (when excited by blue light), as shown in the figure. The resolution in the luminescent patterns is less than 1 μm, limited mainly by diffraction effects as explained in [8]. A similar result is obtained by exposing a LiF film (1 μm thick) rather than a crystal, as shown in Fig. 17. In spite of the fact that the LiF film has been coated with a 50 nm glass layer, still the resolution is much below 1 μm.
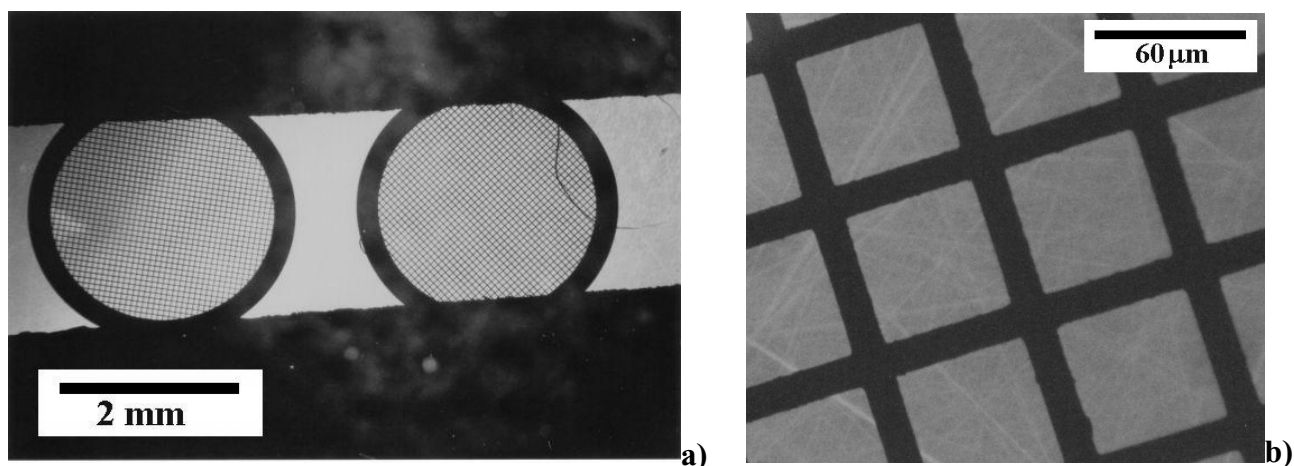
Figure 16: LiF crystal exposed to EUV through a copper mesh, here observed both directly (a) and under an optical microscope with a 40X objective (b). In this case the microscope is a conventional one (not a fluorescence one) with a yellow filter behind the objective and the excitation in the blue is obtained by illuminating directly the LiF by an expanded Ar laser at 458 nm.

Another technique for the generation of luminescent patterns consists on writing the patterns by e-beams[2], but salts like LiF are insulators and hence charge-space effects appear and low e-beam current values must be used; the main advantage of the use of EUV radiation is that large areas (some square centimeters) can be treated at sub-micron resolution with exposure-times orders of magnitude lower than for e-beam direct writing: in our case by operating the laser at 10 Hz it is possible to reach the proper exposure of the LiF plate (~ 100 mJ/cm^2) over some centimeters area in less than two minutes. This time is some orders of magnitude lower than for e-beam writing[2].
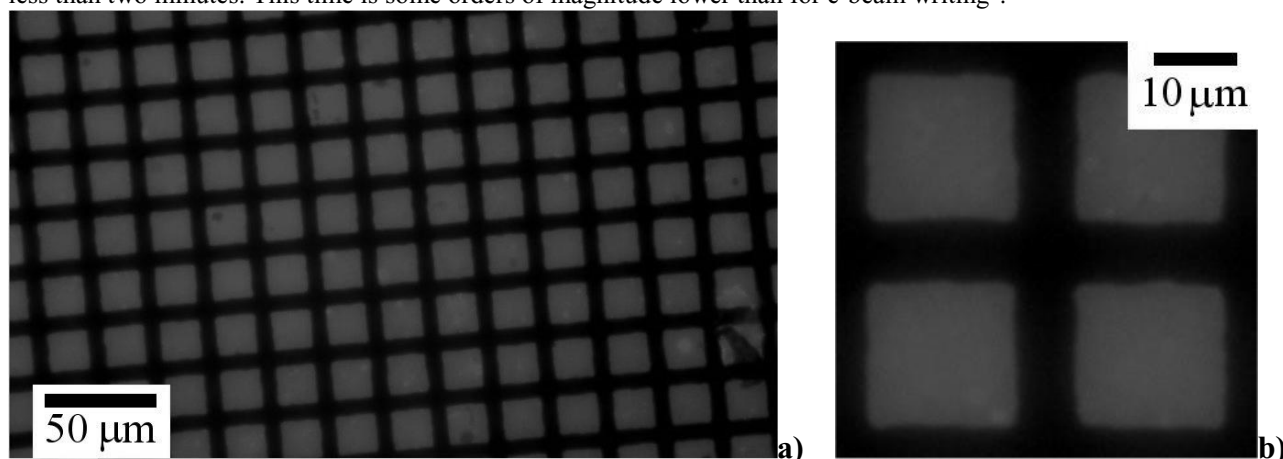

Figure 17: Radiography of a 1000 lpi copper mesh on a 1 μm LiF film coated with 50 nm SiO$_2$ layer. The exposure is obtained by 700 shots of our plasma source placing the sample at 7 cm from the source. The LiF is here observed at a confocal optical microscope (in fluorescence mode) having a 40X objective (a). A zoom of the image is also shown (b).

4. CONCLUSIONS AND ACKNOWLEDGMENTS

EUV and soft-X rays produced by laser plasmas or by X-ray lasers can efficiently generate color centers in alkali halide crystals; the coloration efficiency is much larger than when using conventional X-ray tubes. The penetration depth is typically much smaller than 1 μm and consequently, after the exposure, the LiF surface can be analyzed with high resolution optical microscopes (like confocal or SNOM) and a resolution of 100 nm or less can in principle be reached. This fact, together with the high dynamic range, makes LiF a very promising detector for micro-radiography, X-ray contact microscopy and X-ray laser beams diagnostic. Preliminary results of such applications have been shown here. Due to the response of the CCs density vs X-ray dose shown in Fig. 8, images of 10-12 bits (that is with more than 1000

gray levels) can be obtained and no development is needed after the exposure to X-rays, while by using PMMA[16,18,19] the dynamic range is limited by the development process so that the final dynamic in the images is limited to 5-6 bits. The problem of the contrast dynamic is much smaller when photographic films are used but, in this case, the emulsion grains size limits the resolution to few microns. The use of LiF as detector for EUV and soft X-ray imaging is an ENEA pending patent[25].

Large areas of LiF crystals or films (some cm^2) have been patterned at high resolution (< 1μm) with the EUV radiation produced by our laser-plasma source and the treatment rate has resulted to be some orders of magnitude faster than for e$^-$ -beams treatment. This result is very interesting for applications of LiF to photonics. In particular, the high resolution and the generation of a patterned population inversion in LiF crystals or films allow for example to obtain distributed feedback (DFB) lasers where a periodical structure colored/uncolored must be generated. These are mirrorless laser devices in which the feedback mechanism is distributed throughout and integrated with the gain medium Since the period of the grating in a DFB must be one quarter of the lasing wavelength, this means that it should be in the range 130-190 nm in order to obtain a DFB lasing in the visible spectrum, where F_2 and F_3^+ CCs gives the highest gain values; such a structure could be easily reached by interference of an X-ray laser (see for example Fig. 14b) . A DFB laser action at 680 nm has already been observed by pumping a LiF:F_2 crystal[26].

The applications of LiF in photonics are rather wide: Integrated optical or electro-optical and photonic Microsystems, Amplifiers, Miniaturised coherent light sources, Highly directional and multi-wavelength LEDs, Microlasers, DFB, Gratings, Optical data storage, etc. The present work contains preliminary results in this new field, and future improvements are expected.

5. REFERENCES

1. J.H. Schulman and W.D. Compton: "Color Centers in Solids", Pergamon Press, 1962.

2. E.J. Caine and S.D. Miller: "Optical data storage in LiF using electron beam encoding", J. Vac. Sci. Technol. B , Vol. 16 (6), pp. 3232-3236, (1998).

3. R.M. Montereali: "Colour centres in thin alkali halide films for optical Microsystems", Rad. Eff. Def. Solids, Vol. 149, 189 (1999).

4. R.M. Montereali, M. Piccinini, and E. Burattini: "Amplified spontaneous emission in active channel waveguides produced by electron-beam lithography in Li Fcrystals", App. Phys. Lett. (26), Vol. 78, 4082-4084 (2001).

5. A. Belarouci et al.: "Spontaneous emission properties of color centers based optical microcavities" , Opt. Commun. Vol. 189, p. 281-287, (2001).

6. P. Adam et al. "Fluorescence imaging of submicrometric lattices of colour centres in LiF by an aperturless scanning near-field optical microscope", Opt. Express , Vol. 9, pp. 353-359 (2001).

7 S.K. Sekatskii and V.S. Letokhov: "Single fluorescence centers on the tips of crystal needles: First observation and prospects for application in scanning one-atom fluorescence microscopy", Appl. Phys. B, Vol. 63, pp. 525-530, (1996).

8 G. Baldacchini et al.: "High-contrast photoluminescent patterns in lithium fluoride crystals produced by soft X-rays from a laser-plasma source", Appl. Phys. Lett., Vol. 80, pp. 4810-4812 , (2002).

9. R.H. Stulen and D.W. Sweeney: "Extreme ultraviolet lithography", IEEE J. Of Quant. Electr. (5), Vol. 35, pp. 694-699 (1999).

10. David Attwood: "Soft X-rays and Extreme Ultraviolet Radiation: principles and applications", Cambridge University Press, Trumpington Street, Cambridge UK (1999).

11. G. Baldacchini: "Colored LiF: an optical material for all seasons", Journal of Luminescence, Vol. 100, pp. 333-343, 2002.

12. G.Baldacchini, F.Menchini, R.M.Montereali : "Concentration Quenching of the Emission of F_3^+ and F_2 Color Centers in LiF", Rad. Eff.&Def.Solids, Vol. 156, pp. 71-75, (2001).

13. G.Baldacchini, S.Bigotta and R.M.Montereali: "Emission Decay Times of F_2 Color Centers in Heavily Irradiated LiF Crystals", J.Lumin. 94-95, pp. 299-303, (2001).

14. B.L. Henke, E.M. Gullikson and J.C. Davis, "X-ray interactions: photoabsorption, scattering, transmission and reflection at E=50-30000 eV, Z=1-92", Atomic Data and Nucl. Data Tables 54, 181 (1993).

15. Website: http://cindy.lbl.gov/optical_constants/

16. S. Bollanti et al.: "Soft X-ray plasma source for atmospheric pressure microscopy, radiobiology and other applications" , Il Nuovo Cimento , Vol. 20 D, pp. 1685-1701, (1998).

17. G. Baldacchini et al.. "Influence of LiF film growth conditions on electron induced color center formation", Nuclear Instruments and Methods in Physics Research B Vol. 116, pp. 447-451, (1996).

18. P. Albertano et al.: "X-ray contact microscopy using an excimer laser plasma source with different tatget materials and laser pulse durations", J. of Microscopy, vol. 187, Pt.2, pp. 96-103, (1997).

19. Robin A. Cotton: "Soft X-ray contact microscopy: a new technique for the life-sciences", Microcopy and Analysis, pp. 15-17, Sept. 1992.

20. C.H. Skinner et al. : "Contact microscopy with a soft X-ray laser", J. of Microscopy, Vol. 159, pp. 51-60, (1990).

21. T.AQ. Pikuz et al.: « Shadow monochromatic backlighting: large-field high resolution X-ray shadowgraphy with improved spectral tenability", Laser and Particle Beams, Vol. 19, pp. 285-293, (2001).

22. G. Tomassetti et al.: "Capillary discharge soft X-ray lasing in the Ne-like Ar pumped by long current pulses", European Phys. J. D, Vol. 19, pp.73-77, (2002).

23. A. Ritucci et al.: "Sub-milliradiant divergence soft-X-ray laser by active plasma waveguiding in Z-pinch capillary-discharge", accepted for publication on Europhysics Letters, (2003).

24. G. Tomassetti et al.: "High-resolution imaging of a soft-X-ray laser beam by color-centers excitation in lithium fluoride crystals", accepted for publication on Europhysics Letters, (2003).

25. G. Baldacchini et al.: "Method for micrometric and sub-micrometric imaging by irradiation with ionizing radiation through a mask or through a biological sample", ENEA patent pending, deposited on July 2nd 2002, n° TO2002A000575.

26. T. Kurobori, K. Inabe and N. Takeuchi: "Room temperature visible distributed-feedback colour centre laser", J. of Phys. D , Vol. 16, pp. L121-L123, (1983).